Research Paper
Computational Methods for Differential Equations
http://cmde.tabrizu.ac.ir
Vol. 13, No. 3, 2025, pp. 1012-1021
DOI:10.22034/cmde.2024.61040.2619

Numerical solution of the two-dimensional nonlinear Schrödinger equation using an alternating direction implicit method

Endalew Getnet Tsega
Department of Mathematics, College of Science, Bahir Dar University, Bahir Dar, Ethiopia.

Abstract

In this paper, an alternating direction implicit (ADI) finite difference scheme is proposed for solving the two-dimensional time-dependent nonlinear Schrödinger equation. In the proposed scheme, the nonlinear term is linearized by using the values of the wave function from the previous time level at each iteration step. The resulting block tridiagonal system of algebraic equations is solved using the Gauss-Seidel method in conjunction with sparse matrix computation. The stability of the scheme is analyzed using matrix analysis and is found to be conditionally stable. Numerical examples are presented to demonstrate the efficiency, stability, and accuracy of the proposed scheme. The numerical results show good agreement with exact solutions.

Keywords. Nonlinear Schrödinger equation, Time-dependent, Two-dimensional, ADI method, Block tridiagonal system, Sparse matrix, Gauss-Seidel method.

2010 Mathematics Subject Classification. 35Q41, 65M06, 65J15.

1. Introduction

The nonlinear Schrödinger equation is widely used to describe several physical phenomena in various fields of science and engineering, including quantum mechanics, plasma physics, nonlinear optics, water waves, bimolecular dynamics, and electromagnetic propagation [5, 6, 22]. The nonlinear Schrödinger equation in two-dimension can be written in the following form [4]:

$$i\frac{\partial u(x,y,t)}{\partial t}+\alpha\frac{\partial^2 u(x,y,t)}{\partial x^2}+\frac{\partial^2 u(x,y,t)}{\partial y^2}+\beta\left|u(x,y,t)\right|^2 u(x,y,t)+p(x,y)u(x,y,t)=0,\quad (x,y)\in\Omega,\ t\in(0,T),\ (1.1)$$

with the initial condition

$$u(x,y,0)=f(x,y),\qquad (x,y)\in\Omega,$$

and the boundary condition $u(x,y,t)=g(x,y,t),\ (x,y)\in\partial\Omega$, and $t\in(0,T)$, where $u(x,y,t)$ is the complex-valued wave function, $i=\sqrt{-1}$, $\Omega=[a,b]\times[c,d]\subset\mathbb{R}^2$, $\partial\Omega$ is the boundary of Ω, a and b are real constants, f and g are sufficiently smooth functions. The function $p(x,y)$ is a real-valued and bounded potential function defined on Ω.

Due to the importance of the nonlinear Schrödinger equation for describing several physical phenomena, finding a solution to the equation is essential. Analytical solutions of the nonlinear Schrödinger equation are difficult to obtain [7, 8, 18, 19], and thus numerical techniques are widely used. Several numerical methods have been proposed by researchers to solve the nonlinear Schrödinger equation. Xu and Zhang [24] presented four ADI schemes for solving the two-dimensional nonlinear Schrödinger equation. The authors confirmed the stability of the numerical schemes and compared their accuracy and CPU time through numerical experiments. Bratsos [2] presented a linearized finite difference method to obtain the solution of nonlinear Schrödinger equation. The author replaced the nonlinear term with a parameterized linearized expression based on Taylor's expansion. Lin et al. [16] performed numerical simulations of the nonlinear Schrödinger equation using the implicit-Euler scheme and approximated the unknown function using

Received: 30 March 2024 ; Accepted: 13 August 2024.
Corresponding author. Email: endalebdumath2016@gmail.com.

Gaussian radial basis functions. They verified the efficiency and stability of the numerical scheme through numerical experiments and quantified the error in solving 3D nonlinear Schrödinger problems. Eskar et al. [6] presented a high-order compact finite difference method for solving the nonlinear Schrödinger equation. The authors demonstrated that these schemes maintain conservation laws and offer precise and stable solutions for linear and nonlinear 3D Schrödinger equations. Cavalcanti et al.[3] applied a finite difference scheme to solve a higher-order nonlinear Schrödinger equation. This scheme is designed to uphold the numerical L_2 norm and regulate energy based on the chosen parameters of the equation.

Shivanian and Jafarabadi [21] used spectral meshless radial point interpolation technique for solving two-dimensional nonlinear Schrödinger equation. The authors applied a predictor-corrector method to eliminate nonlinearity. They demonstrated the stability and convergence of the numerical method and validated its accuracy through numerical examples. Pathak et al. [20] introduced a simple, stable, efficient, and accurate numerical technique, the Kansa method with polyharmonic radial basis function, for solving generalized 2D nonlinear Schrödinger equations, supported by stability analysis. Jiwari et al. [14] used a meshfree approach to solve the nonlinear Schrödinger equation. The authors employed the local radial basis function-based differential quadrature method to reduce the problem of ill-conditioning. Karabaş et al. [15] used the meshless method with radial basis functions based on the Fréchet derivative to solve the nonlinear Schrödinger equation.

Iqbal et al. [12] applied the cubic B-spline Galerkin method to solve the Schrödinger equation. The efficiency and accuracy of the method were evaluated using three different cases: a single solitary wave, the collision of two solitary waves, and the collision of three solitary waves. Arora et al. [1] used trigonometric cubic B-spline basis function with the differential quadrature method to simulate nonlinear Schrödinger equations. This method transforms the nonlinear equation into a collection of ordinary differential equations, which can then be solved using the Runge-Kutta method. The obtained numerical results were found to closely match the exact solution. He and Lin et al. [9] used the Lattice Boltzmann method for analysis and simulation of coupled nonlinear Schrödinger equation. The numerical results obtained using this method were compared with those from the finite difference and analytical methods to validate its efficiency. Ismail [13], Hu [10], Iqbal et al. [11], and Wang and Li [23] used different approaches of the finite element method to solve the nonlinear Schrödinger equation. Dehghan et al. [4] used the time-space pseudo-spectral method to find the solution of the nonlinear Schrödinger equation. The authors verified that this method offers a satisfactory approximation even with a relatively small number of points. Liu et al. [17] applied Harr wavelets multi-resolution collocation procedures to solve nonlinear Schrödinger equations. Stability analysis of the proposed methods was conducted, indicating their accuracy and efficiency in time compared to other methods.

Several authors have used different techniques to develop linearized numerical schemes to solve the nonlinear Schrödinger equation. As far as the authors are aware, some of the linearization techniques require lengthy procedures for the formulation of the numerical schemes. The aim of this work is to develop an alternating direction implicit scheme by replacing the nonlinear term with values of the unknown variable from the previous the time level, and to investigate its practicality for solving nonlinear Schrödinger equation. The numerical scheme has been tested by solving different nonlinear Schrödinger equations.

2. Numerical Scheme

In this study, an alternating direction implicit scheme is used to solve (1.1). This scheme involves two stages of solving block tridiagonal systems of equations along the lines parallel to the x- and y-axes. To solve Eq. (1.1) with the scheme, we divide the interval $[a, b]$ into N_x subintervals with step size Δx, the interval $[c, d]$ into N_y subintervals with step size Δy and time interval $[0, T]$ into N_t subintervals with step size Δx. The grid points of the subdivisions are

$$\begin{aligned}
&x_1, x_2, ..., x_{Nx} + 1, && x_1 = a, x_{Nx} + 1 = b, && x_j = x_1 + (j-1)\Delta x, && j = 2, 3, ..., Nx,\\
&y_1, y_2, ..., y_{Ny} + 1, && y_1 = c, y_{Ny} + 1 = d, && y_k = y_1 + (k-1)\Delta y, && k = 2, 3, ..., Ny,\\
&t_1, t_2, ..., t_{Nt} + 1, && t_1 = 0, t_{Nt} + 1 = T, && t_n = t_1 + (n-1)\Delta t, && n = 2, 3, ..., Nt.
\end{aligned}$$

The value of $u(x, y, t)$ at (x_j, y_k, t_n) is approximated as $U^n_{j,k}$ in the numerical approximation. The two stages of the numerical scheme are discussed as follows in the discretization of Eq. (1.1). In the first stage, the derivatives $\frac{\partial u}{\partial t}$, $\frac{\partial^2 u}{\partial x^2}$,

and $\frac{\partial^2 u}{\partial y^2}$ at $(j,k,n+\frac{1}{2})$, $(j,k,n+1)$, and (j,k,n), respectively are approximated by central differences. The nonlinear term and the last term in the left side of Eq. (1.1) are approximated by values of the functions at (j,k,n). From these, we get

$$i\left(\frac{U_{j,k}^{n+1}-U_{j,k}^{n}}{\Delta t}\right)+\alpha\left(\frac{U_{j+1,k}^{n+1}-2U_{j,k}^{n+1}+U_{j-1,k}^{n+1}}{\Delta x^2}+\frac{U_{j,k+1}^{n}-2U_{j,k}^{n}+U_{j,k-1}^{n}}{\Delta y^2}\right)+\beta\left|U_{j,k}^{n}\right|^2U_{j,k}^{n}+p_{i,j}U_{j,k}^{n}=0,$$

or

$$r_xU_{j-1,k}^{n+1}+(i-2r_x)U_{j,k}^{n+1}+r_xU_{j+1,k}^{n+1}=-r_yU_{j,k-1}^{n}+(i+2r_y-\beta\Delta t\left|U_{j,k}^{n}\right|^2-\Delta tp_{i,j})U_{j,k}^{n}-r_yU_{j,k+1}^{n}, \tag{2.1}$$

where $r_x=\frac{\alpha\Delta t}{\Delta x^2}$ and $r_y=\frac{\alpha\Delta t}{\Delta y^2}$.

In the second stage we advance from $(n+1)^{th}$ to $(n+2)^{th}$ time level to approximate $\frac{\partial^2 u}{\partial y^2}$ at $(j,k,n+2)$ to obtain the discretization of Eq. (1.1) as

$$i\left(\frac{U_{j,k}^{n+2}-U_{j,k}^{n+1}}{\Delta t}\right)+\alpha\left(\frac{U_{j+1,k}^{n+1}-2U_{j,k}^{n+1}+U_{j-1,k}^{n+1}}{\Delta x^2}+\frac{U_{j,k+1}^{n+2}-2U_{j,k}^{n+2}+U_{j,k-1}^{n+2}}{\Delta y^2}\right)+\beta\left|U_{j,k}^{n+1}\right|^2U_{j,k}^{n+1}+p_{i,j}U_{j,k}^{n+1}=0,$$

or

$$r_yU_{j-1,k}^{n+2}+(i-2r_y)U_{j,k}^{n+2}+r_yU_{j+1,k}^{n+2}=-r_xU_{j,k-1}^{n+1}+\left(i+2r_x-\beta\Delta t\left|U_{j,k}^{n+1}\right|^2-\Delta tp_{i,j}\right)U_{j,k}^{n+1}-r_xU_{j,k+1}^{n+1}. \tag{2.2}$$

By finding the truncation errors of the discretizations (2.1) and (2.2), it can be shown that the scheme is first-order accurate in time and second-order accurate in space.

To see the basic form of the matrix equations resulting from (2.1) and (2.2), let us take $N_x=N_y=4$ and $r_x=r_y=r$. The iterative schemes (2.1) and (2.2) yield matrix equations

$$A_{1x}U_x^{n+1}=A_{2x}U_x^{n}+b_{1x}, \tag{2.3}$$

where

$$A_{1x}=\begin{bmatrix} i-2r & r & 0 & 0 & 0 & 0 & 0 & 0 & 0\\ r & i-2r & r & 0 & 0 & 0 & 0 & 0 & 0\\ 0 & r & i-2r & 0 & 0 & 0 & 0 & 0 & 0\\ 0 & 0 & 0 & i-2r & r & 0 & 0 & 0 & 0\\ 0 & 0 & 0 & r & i-2r & r & 0 & 0 & 0\\ 0 & 0 & 0 & 0 & r & i-2r & 0 & 0 & 0\\ 0 & 0 & 0 & 0 & 0 & 0 & i-2r & r & 0\\ 0 & 0 & 0 & 0 & 0 & 0 & r & i-2r & r\\ 0 & 0 & 0 & 0 & 0 & 0 & 0 & r & i-2r \end{bmatrix},$$

$$\mathrm{A}_{2x}=\begin{bmatrix} i+2r-B_{2,2} & 0 & 0 & -r & 0 & 0 & 0 & 0 & 0\\ 0 & i+2r-B_{3,2} & 0 & 0 & -r & 0 & 0 & 0 & 0\\ 0 & 0 & i+2r-B_{4,2} & 0 & 0 & -r & 0 & 0 & 0\\ -r & 0 & 0 & i+2r-B_{2,3} & 0 & 0 & -r & 0 & 0\\ 0 & -r & 0 & 0 & i+2r-B_{3,3} & 0 & 0 & -r & 0\\ 0 & 0 & -r & 0 & 0 & i+2r-B_{4,3} & 0 & 0 & -r\\ 0 & 0 & 0 & -r & 0 & 0 & i+2r-B_{2,4} & 0 & 0\\ 0 & 0 & 0 & 0 & -r & 0 & 0 & i+2r-B_{3,4} & 0\\ 0 & 0 & 0 & 0 & 0 & -r & 0 & 0 & i+2r-B_{4,4} \end{bmatrix},$$

$$B_{j,k}=\beta\Delta t\left|U_{j,k}^{n}\right|^2+\Delta tp_{i,j},$$

$$U_x^{n+1} = \begin{bmatrix} U_{2,2}^{n+1} \\ U_{3,2}^{n+1} \\ U_{4,2}^{n+1} \\ U_{2,3}^{n+1} \\ U_{3,3}^{n+1} \\ U_{4,3}^{n+1} \\ U_{2,4}^{n+1} \\ U_{3,4}^{n+1} \\ U_{4,4}^{n+1} \end{bmatrix}, \quad U_x^n = \begin{bmatrix} U_{2,2}^{n} \\ U_{3,2}^{n} \\ U_{4,2}^{n} \\ U_{2,3}^{n} \\ U_{3,3}^{n} \\ U_{4,3}^{n} \\ U_{2,4}^{n} \\ U_{3,4}^{n} \\ U_{4,4}^{n} \end{bmatrix}, \quad b_{1x} = \begin{bmatrix} -rU_{1,2}^{n+1} \\ 0 \\ -rU_{5,2}^{n+1} \\ -rU_{1,3}^{n+1} \\ 0 \\ -rU_{5,3}^{n+1} \\ -rU_{1,4}^{n+1} \\ 0 \\ -rU_{5,4}^{n+1} \end{bmatrix}, \quad + \quad \begin{bmatrix} rU_{2,1}^{n} \\ -rU_{3,1}^{n} \\ -rU_{4,1}^{n} \\ 0 \\ 0 \\ 0 \\ -rU_{2,5}^{n} \\ -rU_{3,5}^{n} \\ -rU_{4,5}^{n} \end{bmatrix},$$

$$A_{1y}U_y^{n+2} = A_{2y}U_y^{n+1} + b_{1y}, \tag{2.4}$$

where

$$A_{1y} = A_{1x},$$

$$\mathrm{A}_{2y} = \begin{bmatrix} i+2r-C_{2,2} & 0 & 0 & -r & 0 & 0 & 0 & 0 & 0 \\ 0 & i+2r-C_{2,3} & 0 & 0 & -r & 0 & 0 & 0 & 0 \\ 0 & 0 & i+2r-C_{2,4} & 0 & 0 & -r & 0 & 0 & 0 \\ -r & 0 & 0 & i+2r-C_{3,2} & 0 & 0 & -r & 0 & 0 \\ 0 & -r & 0 & 0 & i+2r-C_{3,3} & 0 & 0 & -r & 0 \\ 0 & 0 & -r & 0 & 0 & i+2r-C_{3,4} & 0 & 0 & -r \\ 0 & 0 & 0 & -r & 0 & 0 & i+2r-C_{4,2} & 0 & 0 \\ 0 & 0 & 0 & 0 & -r & 0 & 0 & i+2r-C_{4,3} & 0 \\ 0 & 0 & 0 & 0 & 0 & -r & 0 & 0 & i+2r-C_{4,4} \end{bmatrix},$$

$$C_{j,k} = \beta\Delta t \left|U_{j,k}^{n+1}\right|^2 + \Delta t p_{i,j},$$

$$U_y^{n+2} = \begin{bmatrix} U_{2,2}^{n+2} \\ U_{2,3}^{n+2} \\ U_{2,4}^{n+2} \\ U_{3,2}^{n+2} \\ U_{3,3}^{n+2} \\ U_{3,4}^{n+2} \\ U_{4,2}^{n+2} \\ U_{4,3}^{n+2} \\ U_{4,4}^{n+1} \end{bmatrix}, \quad U_y^{n+1} = \begin{bmatrix} U_{2,2}^{n+1} \\ U_{2,3}^{n+1} \\ U_{2,4}^{n+1} \\ U_{3,2}^{n+1} \\ U_{3,3}^{n+1} \\ U_{3,4}^{n+1} \\ U_{4,2}^{n+1} \\ U_{4,3}^{n+1} \\ U_{4,4}^{n+1} \end{bmatrix}, \quad b_{1y} = \begin{bmatrix} -rU_{2,1}^{n+2} \\ 0 \\ -rU_{2,5}^{n+2} \\ -rU_{3,1}^{n+2} \\ 0 \\ -rU_{3,5}^{n+2} \\ -rU_{4,1}^{n+2} \\ 0 \\ -rU_{4,5}^{n+2} \end{bmatrix} + \begin{bmatrix} -rU_{1,2}^{n+1} \\ -rU_{1,3}^{n+1} \\ -rU_{1,4}^{n+1} \\ 0 \\ 0 \\ 0 \\ -rU_{5,2}^{n+1} \\ -rU_{5,3}^{n+1} \\ -rU_{5,4}^{n+1} \end{bmatrix},$$

The system described in (2.3) and (2.4) can be easily generalized for any mesh size. As observed in the above discussion, the scheme requires solving a block tridiagonal system of equations. The Gauss-Seidel method with sparse matrix computation is applied to solve the system at each stage of the scheme.

3. Stability Analysis

Here, we discuss the stability of the scheme using matrix analysis. Consider the matrices and vectors in (2.3) and (2.4) for any mesh size with $N_x = N_y$. The vectors b_{1x} and b_{1y} contain values of the wave function at the boundaries, and there is no error at the boundaries. Thus, the scheme is stable if the modulus of each eigenvalue of the matrices $A_{1x}^{-1}A_{2x}$ and $A_{1y}^{-1}A_{2y}$ is less than or equal to 1. Let us consider the case when $\beta = 0$ and $p(x, y)$, in which case we have $A_{1x}^{-1}A_{2x} = A_{1y}^{-1}A_{2y}$. The maximum of the modulus of eigenvalues of $A_{1x}^{-1}A_{2x}$ (spectral radii), taking $\Omega = [0, 1] \times [0, 1]$ and $\alpha = 1$ at different spatial and time steps, is presented in Table 1. The corresponding spectral radii for solving the two-dimensional heat equation

$$\frac{\partial T(x, y, t)}{\partial t} = \frac{\partial^2 T(x, y, t)}{\partial x^2} + \frac{\partial^2 T(x, y, t)}{\partial y^2}, \tag{3.1}$$

TABLE 1. Spectral radii of $A_{1x}^{-1}A_{2x}$ for solving the schrödinger equation for different mesh sizes.

$\Delta x \downarrow \Delta t \rightarrow$	0.01	0.005	0.001	0.0005	0.0001
0.1	2.002261	1.479790	1.036043	1.009378	1.000380
0.05	3.981984	2.829080	1.370533	1.130283	1.006262
0.025	7.974991	5.650443	2.543146	1.829717	1.089373

TABLE 2. Spectral radii of $A_{1x}^{-1}A_{2x}$ for solving heat Equation (3.1) for different mesh sizes.

$\Delta x \downarrow \Delta t \rightarrow$	0.01	0.005	0.001	0.0005	0.0001
0.1	1.625842	0.952198	0.990259	0.995118	0.999022
0.05	3.683124	2.573814	0.990199	0.995087	0.999016
0.025	7.566080	5.431009	2.310299	1.477936	0.999014

using the scheme on the same domain and with the step sizes is shown in Table 2.

From Tables 1 and 2, it is observed that the scheme is conditionally stable for solving the two-dimensional Schrödinger and heat equations.

4. Numerical Results and Discussions

In this section, numerical examples are provided to demonstrate the efficiency and accuracy of the numerical scheme. Comparisons between the numerical and exact solutions are presented graphically. In the examples, equal numbers of grid points on the x-axis and y-axis are used, i.e., $N_x = N_y = N$. $R(x, y, t)$ and $I(x, y, t)$ represent the real and imaginary parts of u, respectively. The accuracy of the numerical scheme is tested using the absolute maximum error

$$E = \max_{1\leq j,k\leq N} \left|u(x_j, y_k, t_n) - U_{j,k}^n\right|, \tag{4.1}$$

where $u(x_j, y_k, t_n)$ and $U_{j,k}^n$ are the exact and numerical solutions of u, respectively. The computations are carried out using MATLAB code on a PC with Windows 10 OS (64-bit), Intel(R) Core i7-7500U, CPU @ 2.9 GHz, and 8GB RAM.

Example 4.1. Consider a two-dimensional nonlinear Schrödinger equation, (1.1), with $\alpha = 1$, $\beta = 2\pi^2 - 1$ and potential function $p(x, y) = (2\pi^2 - 1)(1 - cos^2\pi x cos^2\pi y)$ [21]. The initial and boundary conditions are obtained from the exact solution $u(x, y, t) = \cos\pi x \cos\pi y e^{-it}$.

The equation is solved on $\Omega = [0, 1] \times [0, 1]$ for $t > 0$. Figure 1 shows the surface plot of the numerical and exact solutions of Example 4.1 at $t == 1$ using $N = 40$, $T = 1$, and $\Delta t = 0.005$. The maximum absolute errors for the real part and imaginary part are $2.4933e - 04$ and $1.811e - 04$, respectively. From the computational results, the solutions at $y = 0.2$ are displayed in Figure 2. From the figures, we observe that the numerical solution is in good agreement with the exact solution and is consistent with [21]. In Table 3, the maximum absolute error and CPU time of the scheme are presented for $N = 10$, 20, 40, 80, and $\Delta t = 0.001$. The absolute error decreases as the number of mesh points increases. Table 4 displays the maximum absolute error and CPU time by taking $T = 1$ and $N = 40$ for different time step sizes. These tables confirm the accuracy and convergence of the numerical scheme.

Example 4.2. Consider (1.1) with $\alpha = \frac{1}{2}$, $\beta = -1$, and the potential function $p(x, y) = -1 + \sin^2 x \cos^2 y$ on $\Omega = [0, 2\pi] \times [0, 2\pi]$ for $t > 0$ [24]. The exact solution is $u(x, y, t) = (\sin x \cos x)e^{-2it}$, and the initial and boundary conditions are obtained from this solution. Numerical solution of Example 4.2 is obtained at $t = 1$ with $N = 60$, $T = 1$, and $\Delta t = 0.005$. In the computation, the maximum absolute errors of the scheme for real and imaginary parts are $3.5435e - 3$ and $2.9207e - 3$, respectively. Figure 3 shows a surface plot of numerical and exact solutions for the real and imaginary parts of u. The numerical and exact solutions at the diagonal, connecting the points $(0, 2\pi)$ and $(2\pi, 0)$ of the domain, are displayed in Figure 4. As observed from the figures, the numerical solutions coincide with the exact solution, demonstrating the accuracy of the numerical scheme.

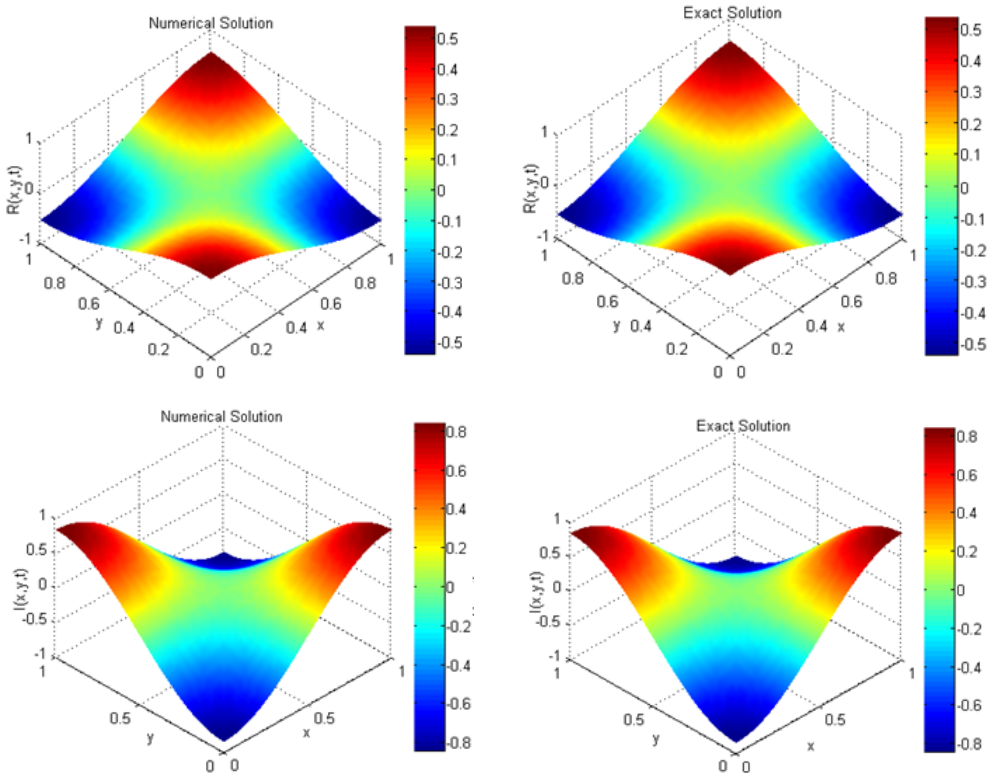

FIGURE 1. Surface plot of numerical and exact solutions for Example 4.1 at $t = 1$ with$N = 40$, $T = 1$, and $\Delta t = 0.005$.

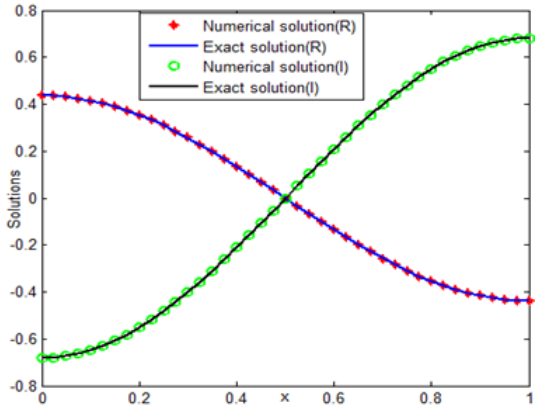

FIGURE 2. Graph of numerical and exact solutions for Example 4.1 at $y = 0.2$ and $t = 1$ with $N = 40$, $T = 1$, and $\Delta t = 0.005$.

Example 4.3. Consider Eq. (1.1) with $\alpha = \frac{1}{2}$, $\beta = 1$ and potential function $p(x, y) = 1 - \sinh x \sinh y - sinh^2 x sinh^2 y$ on $\Omega = [0, 1] \times [0, 1]$ for $t > 0$.The exact solution is $u(x, y, t) = (i \sin x \sinh y)e^{it}$. As in the previous examples, the initial and boundary conditions are computed from the exact solution.

TABLE 3. Maximum absolute errors and CPU times with $\Delta t = 0.001$, $T = 1$, and different mesh sizes for Example 4.1.

N	R E	I E	CPU time(s)
10	1.933832 e-03	1.065042 e-03	22.415811
20	6.296480e-04	6.811864e-04	148.841399
40	2.385183e-04	1.441837e-04	3035.401684
80	1.717893e-04	6.176003e-06	38047.729067

TABLE 4. Maximum absolute errors and CPU times with$N = 40$, $T = 1$, and different time step sizes for Example 4.1.

N_t	R E	I E	CPU time(s)
10	9.715348 e-03	5.730540 e-03	29.520303
50	2.223621 e-03	7.149175e-04	162.029855
100	1.029718e-03	4.836240e-04	223.20477
1000	2.385183e-04	1.441837e-04	3035.401684

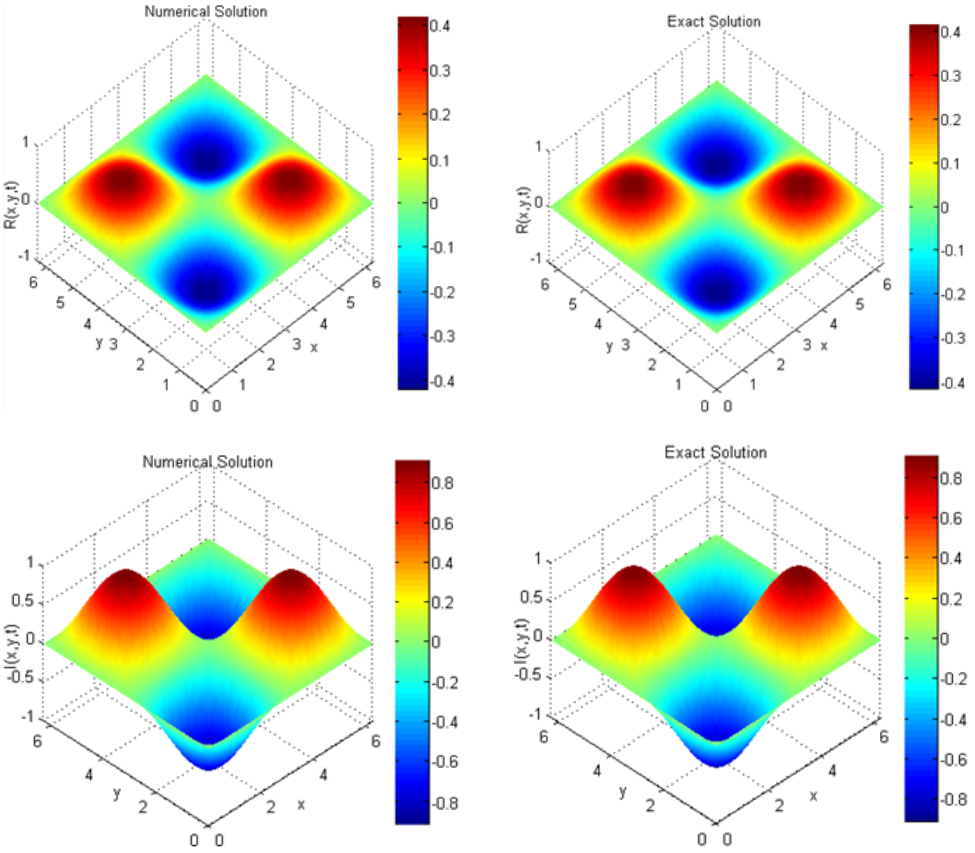

FIGURE 3. Surface plot of numerical and exact solutions for Example 4.2 at $t = 1$ with $N = 60$, $T = 1$, and $\Delta t = 0.005$.

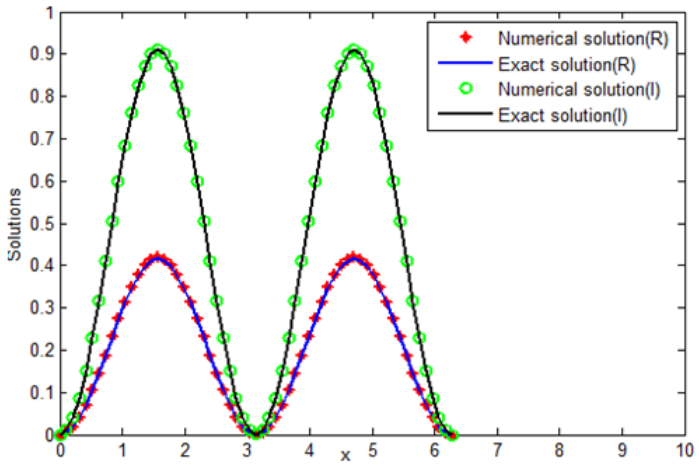

FIGURE 4. Graph of numerical and exact solutions for Example 4.2 along the diagonal of the domain (joining the points $(0, 2\pi)$ and $(2\pi, 0)$) at $t = 1$ with $N = 60$, $T = 1$, and $\Delta t = 0.005$.

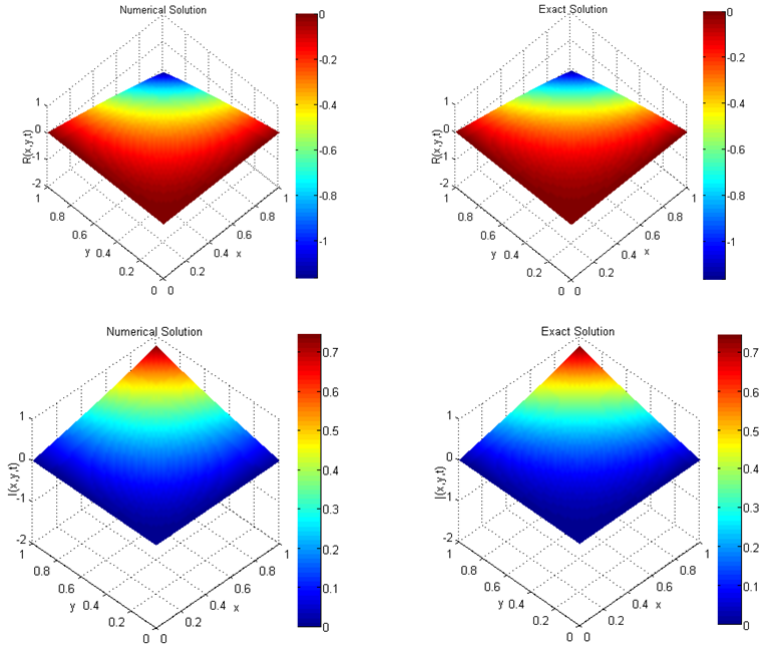

FIGURE 5. Surface plot of numerical and exact solutions for Example 4.3 at $t = 1$ with $N = 50$, $T = 1$, and $\Delta t = 0.005$.

For computational work, $N = 50$, $T = 1$, $\Delta t = 0.005$, and $t = 1$ are used. Surface plots of numerical and exact solutions of the real and imaginary parts are presented in Figure 5. For better visualization, the graphs of numerical and exact solutions along the diagonal, connecting the points $(0, 0)$ and $(1, 1)$, are displayed in Figure 6. These figures show that the numerical results are in good agreement with the exact solutions.

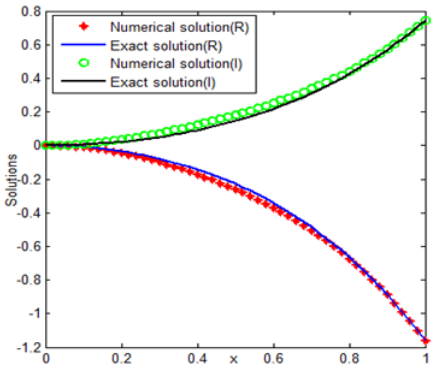

FIGURE 6. Graph of numerical and exact solutions for Example 4.3 along the diagonal (from $(0,0)$ to $(1,1)$) at $t = 1$ with $N = 50$, $T = 1$, and $\Delta t = 0.005$.

5. Conclusion

In this work, an alternating direction implicit numerical scheme is presented for solving a two-dimensional nonlinear Schrödinger equation. The Gauss-Seidel method is used to solve the system of algebraic equations resulting from the discretization. The stability of the numerical scheme is analyzed and found to be conditionally stable. The efficiency and accuracy of the scheme are demonstrated using three test examples. The obtained numerical results are compared with exact solutions and it is observed that all results are in close agreement to the exact solutions.

Conflict of Interests

The author declares no conflict of interest.

References

[1] G. Arora, V. Joshi, and R. C. Mittal, *Numerical simulation of nonlinear Schrödinger equation in one and two dimensions*, Mathematical Models and Computer Simulations,*11*(4) (2019), 634-648.

[2] A. G. Bratsos, *A linearized finite-difference scheme for the numerical solution of the nonlinear cubic Schrödinger equation*, Korean Journal of Computational and Applied Mathematics, *8*(2001), 459-467.

[3] M. M. Cavalcanti, W. J. Corrêa, M. A. Sepúlveda C, and R. Véjar-Asem, *Finite difference scheme for a higher order nonlinear Schrödinger equation*, Calcolo,*56*(4) (2019), 40.

[4] M. Dehghan and A. Taleei, *Numerical solution of nonlinear Schrödinger equation by using time-space pseudo-spectral method*, Numerical Methods for Partial Differential Equations: An International Journal, *26*(4) (2010), 979-992.

[5] R. K Dodd, J. C. Eilbeck, and J. D. Gibbon, *Solitons and Nonlinear Wave Equations*, New York: Academic Press, 1982.

[6] R. Eskar, P. Huang, and X. Feng,*A new high-order compact ADI finite difference scheme for solving 3D nonlinear Schrödinger equation*, Advances in Difference Equations, *2018:286* (2018).

[7] L. Guo, Y. Guo, S. Billings, D. Coca, and Z. Lang,*The use of Volterra series in the analysis of the non-linear Schrödinger equation*, Nonlinear Dynamics, *73*(3) (2013), 1587-1599.

[8] Q. Guo and J. Liu, *New exact solutions to the nonlinear Schrödinger equation with variable coefficients*, Results in Physics, *16* (2020), 102857.

[9] Y. He and X. Lin, *Numerical analysis and simulations for coupled nonlinear Schrödinger equations based on lattice Boltzmann method*,Applied Mathematics Letters, *106* (2020), 106391.

[10] H. Hu, *Two-grid method for two-dimensional nonlinear Schrödinger equation by finite element method*, Numerical Methods for Partial Differential Equations, *34*(2) (2018), 385-400.

[11] A. Iqbal, N. N. Abd Hamid, and A. I. M. Ismail, *Numerical solution of nonlinear Schrödinger equation with Neumann boundary conditions using quintic B-spline Galerkin method*, Symmetry, *11*(4) (2019), 469.
[12] A. Iqbal, N. N. Abd Hamid, and A. I. M. Ismail, *Cubic B-spline Galerkin method for numerical solution of the coupled nonlinear Schrödinger equation*, Mathematics and Computers in Simulation, *174* (2020), 32-44.
[13] M. S. Ismail, *Numerical solution of coupled nonlinear Schrödinger equation by Galerkin method*, Mathematics and Computers in Simulation, *78*(4) (2008), 532-547.
[14] R. Jiwari, S. Kumar, R. C. Mittal, and J. Awrejcewicz, *A meshfree approach for analysis and computational modeling of non-linear Schrödinger equation*, Computational and Applied Mathematics, *39* (2020), 1-25.
[15] N. İ. Karabaş, S. Ö. Korkut, G. Tanoğlu, and I. Aziz,*An efficient approach for solving nonlinear multidimensional Schrödinger equations*, Engineering Analysis with Boundary Elements, *132* (2021), 263-270.
[16] J. Lin, Y. Hong, L. Ku, and C. Liu, *Numerical simulation of 3D nonlinear Schrödinger equations by using the localized method of approximate particular solutions*, Engineering Analysis with Boundary Elements, *78* (2017), 20-25.
[17] X. Liu, M. Ahsan, M. Ahmad, I. Hussian, M. M. Alqarniand, and E. E.Mahmoud, *Haar wavelets multi-resolution collocation procedures for two-dimensional nonlinear Schrödinger equation*, Alexandria Engineering Journal, *60*(3) (2021), 3057-3071.
[18] W. X. Ma and M. Chen, *Direct search for exact solutions to the non-linear Schrödinger equation*, Applied Mathematics and Computation, *215*(8) (2009), 2835-2842.
[19] G. Q. Meng, Y. T. Gao, X. Yu, Y. J. Shen, and Y. Qin, *Multi-soliton solutions for the coupled non-linear Schrödinger-type equations*, Nonlinear Dynmics, *70*(1) (2012), 609-617.
[20] M. Pathak, P. Joshi, and , K. S. Nisar, *Numerical study of generalized 2-D nonlinear Schrödinger equation using Kansa method*, Mathematics and Computers in Simulation, *200* (2022), 186-198.
[21] E. Shivanian and A. Jafarabadi, *An efficient numerical technique for solution of two-dimensional cubic nonlinear Schrödinger equation with error analysis*, Engineering Analysis with Boundary Elements, *83* (2017), 74-86.
[22] C. Sulem and P. L. Sulem, *The Nonlinear Schrödinger Equation: Self-Focusing and Wave Collapse*, New York: Springe, 1999.
[23] L. Wang and M. Li, *Galerkin finite element method for damped nonlinear Schrödinger equation*, Applied Numerical Mathematics, *178* (2022), 216-247.
[24] Y. Xu and L. Zhang,*Alternating direction implicit method for solving two-dimensional cubic nonlinear Schrödinger equation*, Computer Physics Communications, *183* (2012), 1082-1093.